Biochemical Pharmacology 82 (2011) 977–983

Contents lists available at ScienceDirect

Biochemical Pharmacology

journal homepage: www.elsevier.com/locate/biochempharm

Acute in vivo nicotine administration enhances synchrony among dopamine neurons

Wei Li [b], William M. Doyon [a], John A. Dani [a,*]

[a] Center on Addiction, Learning, Memory, Department of Neuroscience, Menninger Department of Psychiatry and Behavioral Sciences, Baylor College of Medicine, Houston, TX 77030, United States
[b] Diana Helis Henry Medical Research Foundation, New Orleans, LA 70130, United States

ARTICLE INFO

Article history:
Received 2 May 2011
Accepted 2 June 2011
Available online 12 June 2011

Keywords:
Nicotinic acetylcholine receptors
Mesolimbic
Ventral tegmental area
Nicotine addiction
Synchronization
Correlation

ABSTRACT

Altered functional interactions among midbrain dopamine (DA) neurons contribute to the reinforcing properties of environmental stimuli and addictive drugs. To examine correlations among DA neurons, acute nicotine was administrated to rats via an intraperitoneal catheter and unit activity was measured using multi-tetrode in vivo recordings. Nicotine administration enhanced the correlated activity of simultaneously recorded DA neurons from the ventral tegmental area (VTA). The strength of the correlations between DA neuron pairs, as measured by cross covariance among two spike trains, showed dynamic changes over time. Nicotine produced a gradual rise in firing rate and burst activity that reached a stable plateau approximately 20 min after the intraperitoneal nicotine infusion. Shortly after that time the cross correlations measured using 5-ms bins increased significantly above baseline. In addition, nicotine increased the firing rates of DA neurons in the posterior VTA more than in the anterior VTA. Unlike nicotine, eticlopride administration also boosted DA neuron firing activity but did not enhance synchronization, indicating that the cross correlations induced by nicotine were not due to a non-specific increase in firing rate. The overall results show that nicotine induces nearly synchronous firing by a subset of DA neurons, and those changes in correlative firing will enhance the DA signal that contributes to nicotine-induced behavioral reinforcement.

1. Introduction

The involvement of dopamine (DA) neurons in learning and incentive based behavior is well known [1,2]. Accumulating evidence indicates that drugs of abuse, such as nicotine, capitalize on the brain's normal reinforcement mechanisms mediated in part by the midbrain DA system. Nicotine increases the firing rate and burst activity of ventral tegmental area (VTA) DA neurons [3–8]. Recent studies indicate that nicotine does not activate all VTA DA neurons uniformly. Rather, the sensitivity of DA neurons to nicotine varies, and there are some systematic changes in responsiveness related to anatomical location [9]. In addition, some reinforcement learning models predict a homogenous response and synchronization among DA neurons to optimize their output [10].

It remains unclear how nicotine influences the coordinated network activity of the VTA. Approximately 25% of VTA DA neurons show synchronized firing patterns as measured by cross correlation analysis [11–13], and this percentage increases in response to conditioned (natural) rewards [10]. In addition to DA neurons, the VTA contains other neuronal types. For example, fast-firing GABA neurons project to several forebrain regions [14–16], and they can form local circuit connections with DA neurons through their axon collaterals [17].

The tetrode recording technique provides a reliable method for isolating the firing activity of multiple units simultaneously in freely moving rodents. To assess the synchrony of DA neuron firing caused by nicotine, correlations between spike trains were computed before and during a 60-min recording period following nicotine administration. We show that nicotine produced an increase in DA neuron firing rates and over time enhanced the synchronous firing activity among a subset of DA neurons, as measured by changes in cross-covariance. These findings indicate that nicotine recruits a significant population of VTA DA neurons to increase coordinated DA neurotransmission, which would unite the transmitted DA signal and likely contribute to the influence over learning and memory processes that underlie nicotine reinforcement [18].

Abbreviations: ACh, acetylcholine; DHβE, dihydro-β-erythroidine; DA, dopamine; ISI, interspike interval; nAChR, nicotinic acetylcholine receptor; NAc, nucleus accumbens; SNc, substantia nigra compacta; VTA, ventral tegmental area.

* Corresponding author. Tel.: +1 713 798 3710; fax: +1 713 798 3946.
E-mail addresses: jdani@bcm.edu, jdani@cns.bcm.edu, jdani@bcm.tmc.edu (J.A. Dani).

0006-2952/$ – see front matter © 2011 Elsevier Inc. All rights reserved.
doi:10.1016/j.bcp.2011.06.006

2. Materials and methods

2.1. Animal care and surgical procedure

Male Long-Evans rats (300–450 g) were housed individually and kept on a 12/12 h light–dark cycle with food and water available ad libitum. All procedures were conducted following the guidelines of the NIH and the Institutional Animal Care and Use Committee at Baylor College of Medicine.

Rats were injected with sodium pentobarbital (Sigma–Aldrich, St. Louis, MO, USA) (40 mg/kg) initially and then maintained with isoflurane anesthesia (2–3% in 100% oxygen, 1 L/min) for the duration of the surgery. Body temperature was maintained with a thermostatically controlled heating blanket. To avoid handling related stress during the experiments, the animals were implanted with an intraperitoneal (i.p.) catheter. Using a stereotaxic apparatus, we implanted a custom made micro-drive (weighing ≈ 20 g) for in vivo unit recording. The micro-drive had 18 independently movable tetrodes positioned to enter the brain (coordinates in mm relative to bregma: −5.6 A–P, 1.0–2.0 M–L). The micro-drive and the catheters (for i.p. infusion of drugs) were fixed to the skull using stainless steel screws and dental cement. The cannulae were flushed with saline daily after implantation to maintain patency and to habituate the animals to the infusions.

2.2. In vivo tetrode unit recordings from midbrain neurons

Tetrodes were constructed from insulated nickel–chromium wire (12 μm OD per strand). The 4 leads of each tetrode were gold-plated to reduce their impedance to 150–400 KΩ. Over the course of days, the tetrodes were slowly positioned into the midbrain DA area (7.5–9.0 mm beneath the surface of the cortex), and the electrical signals were recorded thereafter (Cheetah system, Neuralynx, Tucson, AZ). During recording the animals were free to move within a circular platform (35 cm in diameter).

The recordings were digitized gap-free at 26.5 or 40 kHz after variable low pass and high pass filtering (50–9000 Hz or 600–6000 Hz), saved onto a computer disk, and analyzed off-line. Spikes were identified and extracted in Matlab (Xtractor by M. Krause and W. Li). Individual unit isolation was achieved using the relative amplitudes of the action potentials on each tetrode channel in combination with other spike waveform parameters (e.g., spike duration and waveform shape). This spike sorting procedure was accomplished using in-house software and software developed by Dr. A. David Redish at University of Minnesota (MClust). The final location of the tetrodes in the midbrain was marked by electrolytic lesions (50 μA × 15 s) and in many cases a fluorescent dye (DiI, Sigma–Aldrich, St. Louis, MO, USA) (see [6]). Postmortem analysis using immunohistochemistry confirmed that the recordings were located in tyrosine hydroxylase positive regions of the midbrain.

2.3. VTA dopamine neuron identification and firing parameters

Putative VTA DA and non-DA neurons were distinguished by a combination of features, including basal firing rate, interspike interval (ISI) variability (skewness), and D2-type receptor pharmacological responses [6,12,19,20]. There has been some controversy for identification of DA neurons [20,21], but there are some DA neurons that are more reliably identifiable [22,23] and our very conservative approach aims to identify a subset of DA neurons [6,8]. The non-DA neurons are composed mainly of GABAergic and glutamatergic neurons in the VTA, but they are not examined in this study. Mean firing rate was calculated by dividing the total number of spikes by the baseline recording period (10 min) prior to drug administration or during the 15–60 min following nicotine administration. The mean percentage of spikes within bursts (% of SWB), burst rate (bursts/s), and burst length (spikes/burst) were calculated using the established criteria of a burst [6,24]. The onset of a burst begins when two spikes of an interspike interval occur less than 80 ms apart, and the burst terminates when the interspike interval exceeds 160 ms. Skewness of the ISI distribution was calculated using an established approach [25].

2.4. Cross-covariance analysis

To quantify the interactions between two simultaneous recorded spike trains, we computed their cross-covariance, which is a measure of how often two signals occur at a given time lag. Stated in another way, the cross-covariance is a measure of the similarity of two spike trains as a function of a small time lag (e.g., a 5 ms "window" in our case). We assume that neuronal spikes trains follow a stochastic point process (e.g. N_i) [26]. The differential increment for process N_i is denoted by $dN_i(t)$ and defined as $dN_i(t) = N_i(t, t + dt)$, which counts the number of events during a small duration, dt, starting at t. The mean intensity, P_i of the point process N_i, is defined as $E\{dN_i(t)\} = P_i\,dt$. The cross-product density, $P_{ij}(\mu)$ of the point processes N_i and N_j is defined as $E\{dN_j(t+\mu),\ dN_i(t)\} = P_{ij}(\mu)\,dt d\mu$ which can be interpreted as a probability of a co-occurrence of N_i during $(t, t + dt)$, and N_j during $(t + \mu, t + \mu + dt)$ [27,28]. The cross-covariance function is defined as $q_{ij}(\mu) = P_{ij}(\mu) - P_iP_j$. If two spikes trains N_i and N_j are independent, $P_{ij}(\mu) = P_iP_j$ and $q_{ij}(\mu) = 0$ [29]. The P_i for a sample of duration R of point process N_i can be estimated by $\hat{P}_i = N_i(R)/R$ which means the total number of events, $N_i(R)$ divided by the duration, R. The variant $J_{ij}(\mu)$ counts the number of occurrences of N_j events falling in a bin of width b, whose midpoint is μ time units away from a N_i event. $P_{ij}(\mu)$ is estimated by $\hat{P}_{ij}(\mu) = J_{ij}(\mu)/bR$. Therefore, $q_{ij}(\mu)$ is estimated by $\hat{q}_{ij}(\mu) = J_{ij}(\mu)/bR - N_i(R)/R \times N_j(R)/R$ and the $\hat{q}_{ij}(\mu) \sim N\{\mu = 0, \sigma^2 = P_iP_j/bR\}$ under the null hypothesis H_0 of spike train independence [29]. Because the variance of $\hat{q}_{ij}(\mu)$ is dependent on a spike train's firing rate, bin size and the duration of observation, we use the standardized cross-covariance defined by $Q_{ij}(\mu) = \sqrt{bR/P_iP_j} \times \hat{q}_{ij}(\mu)$ and the $Q_{ij}(\mu) \sim N\{\mu = 0, \sigma^2 = 1\}$ [29].

We computed the $Q_{ij}(\mu)$ for all DA neuron pairs ($n = 52$) over the time lag, μ, between −250 ms and +250 ms using 5 ms bins. Solid and dotted lines indicate 99.5% and 99.95% confidence limits, respectively, under the hypothesis (H_0) of independence. To identify a significant increase in $Q_{ij}(\mu)$ and to avoid spurious correlations caused by noise, we required three consecutive bins to be above the 99.95% confidence limit before rejecting the H_0, corresponding to a Z value of 3.28. In general, an increase in $Q_{ij}(\mu)$ reflects an increase in coincident spike activity at a given time lag. That is, when the cross-covariance, $Q_{ij}(\mu)$ crosses the 99.95% confidence limit (as in Fig. 4), we take the pair of DA neurons to be firing comparably (or in synchrony). The mean cross-covariance, $mean(Q_{ij}(\mu))$ is denoted as $\bar{Q}(\mu)$ and its peak is used to compare correlation strength. Comparisons between peaks in the mean cross covariance were assessed by two-tailed t tests assuming equal variance.

2.5. Experimental time periods

Recording sessions consisted of the short time during the drug administration and the time after the administration with the following test periods: baseline (≈12 min), saline (≈12 min), nicotine (≈60 min), quinpirole (≈15 min), and eticlopride (≈18 min). Drugs were administered once via an intraperitoneal (i.p.) catheter at the start of each period. Drug doses were as follows: nicotine, 0.4 mg/kg, quinpirole and eticlopride, 1.0 mg/kg. All drugs were purchased from Sigma–Aldrich (St. Louis, MO, USA). One assumption of the cross correlation analysis is a stable spike

firing rate. To obtain stability and avoid artifacts from the drug infusion, we sampled the firing rate from the last 10 min of the saline period, the last 45 min of the nicotine period, and the last 10 min of the quinpirole and eticlopride periods.

3. Results

3.1. Location and identification of VTA neurons

The recordings (146 units) were located within the VTA and in a few cases within the substantia nigra compacta (SNc) for comparison (Fig. 1). The exact location of the recording tetrode was determined by electrolytic lesions and in many cases a fluorescent dye left from the tetrode wires [6]. Putative DA neurons were identified by their low firing rate (1–8 Hz) and their D2-type receptor pharmacology (i.e., inhibition to quinpirole and subsequent reversal by eticlopride), as well as the low variability in their firing patterns (mean skew < 4 in their ISI distribution) (Fig. 2). In contrast, putative non-DA neurons (that had characteristics of GABA neurons) exhibited basal firing rates above 10 Hz and showed D2 pharmacological responses that were generally different from the putative DA neurons (Fig. 2A). Action potential duration was shorter and firing patterns were significantly more variable in putative non-DA neurons (Fig. 2B and C). Although other unidentified neurons were found in the VTA (data not shown), the properties of the putative DA and putative non-DA neurons (with GABAergic characteristics) are consistent with current criteria for the identification of major populations of VTA neurons [15,30,31].

3.2. Differential effects of nicotine on DA neuron firing activity

A control infusion of saline (through the i.p. cannula) did not significantly influence DA neuron firing compared to baseline (time: $F(6, 312) = 0.96$, $p > 0.05$). However, nicotine administration (0.4 mg/kg, i.p. cannula) significantly increased the firing rate of 53 out of 57 putative DA neurons (Fig. 3A and B). In general, the rise in the firing rate began in the first 3 min after the infusion and reached a peak response at approximately 15–20 min thereafter. Nicotine inhibited the firing rate of four putative DA neurons. DA neurons that increased their firing rate to nicotine ($n = 53$) showed a significant increase in burst activity [6], as measured by the percentage of spikes occurring within bursts, burst rate, and burst length (Fig. 3C–E). The non-DA neurons (with GABAergic characteristics), by comparison, displayed heterogeneous responses to nicotine that are not examined further here.

Previous studies in VTA brain slices indicate that DA neurons display anatomical differences in their sensitivity to nicotine [9]. Following the lead of Zhao-Shea et al. [9], we divided the DA units by their respective locations in the anterior and posterior VTA (see Fig. 1) and analyzed their responses to nicotine. Anatomical boundaries were taken directly from the stereotaxic estimates described by Ikemoto [32]. Nicotine enhanced the relative firing rate of putative DA neurons in both the anterior and posterior VTA. However, the magnitude of the increase over time was significantly higher for DA neurons in the posterior VTA compared to the anterior VTA (group × time: $F(20, 1020) = 1.73$, $p < 0.05$) (Fig. 3F). The medial-lateral dimension was not analyzed due to an insufficient sample size of medial units in the posterior VTA.

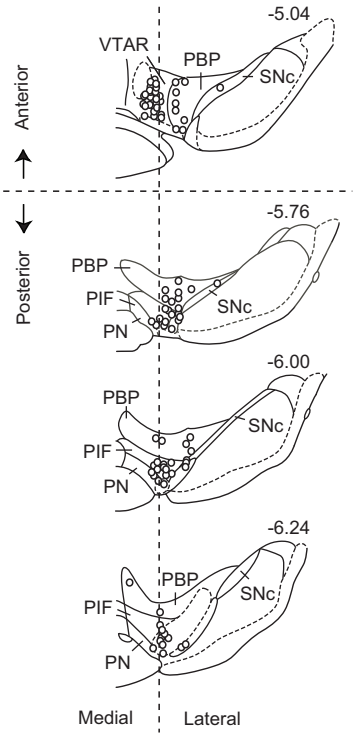

Fig. 1. The approximate location of recordings within the VTA. Recordings were dispersed throughout the VTA with a majority in the parabrachial pigmented nucleus (PBP) and the paraintrafascicular nucleus (PIF). For post hoc analyses, the VTA was subdivided into anterior and posterior regions and medial and lateral regions based on coordinates estimated from previous studies [32]. PN: paranigral nucleus; SNc: substantia nigra pars compacta; VTAR: rostral VTA.
Source: Figure was adapted from [54].

3.3. Nicotine increases DA neuron synchronization

Some reinforcement learning models predict a homogenous response and synchronization among DA neurons to optimize their output [10]. We studied the interactions within the VTA by

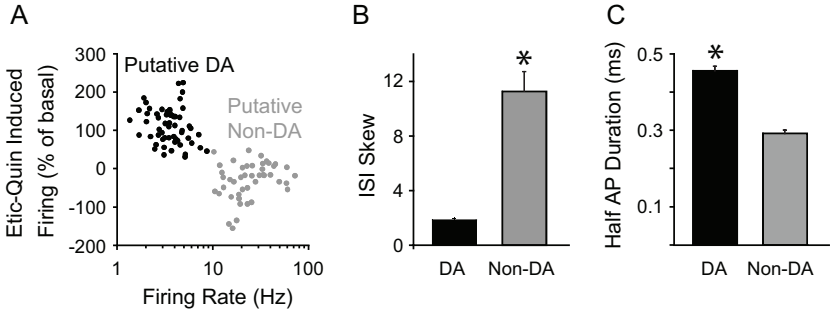

Fig. 2. A combination of features distinguished putative DA neurons and putative non-DA neurons (with GABAergic characteristics). (A) Putative DA and non-DA (with GABAergic characteristics) neurons showed distinct basal firing rates and D2-type receptor pharmacological responses to quinpirole (Quin) and eticlopride (Etic). Etic–Quin is defined as the percent of basal difference between eticlopride-induced firing and quinpirole-induced firing. (B) Putative DA neurons showed low variability in their firing patterns as observed in the interspike interval (ISI) skew and longer action potential durations compared to putative non-DA (with GABAergic characteristics) neurons. $^*p < 0.01$ by paired t-test. A minority of other unidentified units are not shown.

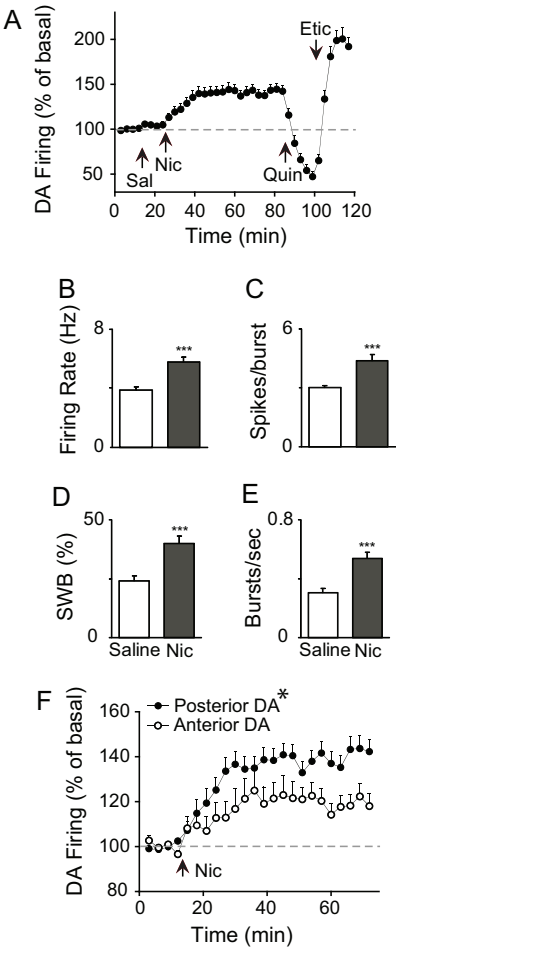

Fig. 3. Effect of saline and nicotine on spontaneous DA neuron firing activity. (A, B) Infusion of nicotine (Nic) via an i.p. catheter, but not saline (Sal), significantly increased the firing rate of putative DA neurons ($n = 53$). The onset of the nicotine effect was gradual but persisted for the duration of the test period. (C–E) Nicotine increased all measures of burst activity, including mean spikes per burst (spikes/burst), percent of spikes occurring within bursts (% of SWB), and burst rate (bursts/s). $^{***}p < 0.001$ by paired t-test. (F) Separation of units based on their anatomical location showed that DA neurons in the posterior VTA were more sensitive to nicotine than anterior VTA DA neurons. $^{*}p < 0.05$ by two-way ANOVA performed on raw data (Hz).

constructing cross correlation histograms for DA neurons that were recorded simultaneously ($n = 52$ pairs). During these recordings, the rats were given non-contingent infusions of saline, nicotine, quinpirole, and eticlopride via an i.p. cannula [8]. Quinpirole is a D2-type receptor agonist that decreases DA neuron firing, and eticlopride is a D2-type receptor antagonist that increases DA neuron firing [6,30,33].

A minority of the DA neurons (21%) showed coordinated firing activity (on a short time scale) at baseline and after saline administration as measured by cross covariance, $Q_{ij}(\mu)$ between neuron pairs using a 5-ms sliding bin (Fig. 4A). Correlations between DA neurons were based on the presence of a peak in the cross covariance spike activity above a set confidence interval (99.95%). The peaks in the cross correlograms were broad (≈100 ms wide) and centered around zero without an apparent time lag, suggesting a shared inhibitory input between the DA neurons [12,34]. A shared inhibitory input is also supported by the fact that some DA neuron pairs ($n = 5$) demonstrated periodicity in their cross correlograms, which was not apparent in the auto-correlograms of the individual neurons (supplemental Fig. S1).

DA neuron pairs were divided into three groups based on their cross covariance during the saline and nicotine epochs (Fig. 4A and B). Type 1 pairs ($n = 11$) showed correlated activity after both saline (control) and nicotine administration. Type 2 pairs ($n = 12$) showed correlated activity only after nicotine administration, indicating that nicotine shifted their activity to a more synchronized state. Type 3 pairs ($n = 29$) showed no correlation in activity in either condition. Therefore, in 44% of the DA neuron pairs, nicotine increased the correlation strength indicative of synchronization.

Eticlopride administration increased the firing rate approximately 80% above baseline (Fig. 2B). However, the cross correlation frequency during this period dropped significantly compared to the nicotine period (Fig. 4B), suggesting that an increase in DA neuron firing was not sufficient to increase correlations or to produce synchronizations. However, the number of cross correlations can depend on the number of events and the length of the sampling period, which was longer for the nicotine epoch (45 min of the 60 min recording) than for the saline or eticlopride epochs (10 min of the 15 min recording).

To observe how the correlations changed within the 60-min recording period for nicotine, we computed the mean cross covariance for DA pairs (Type 1 and Type 2) using a sliding 10-min window (step size, 5 min). These time windows were calculated along the course of the in vivo recording across baseline and administration of saline, nicotine, and eticlopride. Correlations after quinpirole administration were not performed because of the low number of events induced by inhibition. The pseudo-color plots revealed dynamic changes in the $\bar{Q}(\mu)$ of DA neuron pairs during each period (Fig. 5A).

The peak signal of the $\bar{Q}(\mu)$ was highest 30–40 min after the nicotine infusion (indicated by the red color code, Fig. 5A), corresponding to the period after the DA neuron firing rates had reached a plateau. For comparison, the $\bar{Q}(\mu)$ for the three test periods, saline, 30–40 min post nicotine, and eticlopride, are plotted in Fig. 5B. Despite the high firing rates during the eticlopride window (Fig. 5C), the peak signal of the $\bar{Q}(\mu)$ during this period was not significantly different from the saline baseline (Fig. 5D). Therefore, the increase in cross covariance induced by nicotine was not due to an increase in the spike firing rate alone or to the time length used to calculate the correlation. The latter possibility was further confirmed by the lack of a difference between the $\bar{Q}(\mu)$ 30–40 min after nicotine and the $\bar{Q}(\mu)$ for the entire nicotine period (supplemental Fig. S2).

4. Discussion

The reinforcing effects of drugs of abuse, such as nicotine, arise in part from their ability to activate and potentiate VTA DA neurotransmission [2,35,36]. Nicotine influences DA signaling through a complex process of activation and desensitization of nicotinic acetylcholine receptors (nAChRs) located on DA and non-DA neurons and terminals in the VTA [4,6,35,37–41]. Nicotine boosts the single-unit firing activity of midbrain DA neurons within minutes of exposure [3,5,6,8], but nicotine's impact on the coordinated network interactions between DA neurons has only been hypothesized.

We show that in vivo nicotine administration via an i.p. catheter enhances the synchronized activity between pairs of VTA DA neurons recorded simultaneously. Several studies have provided evidence of synchronicity or coupling between DA neurons in their basal state, which occurs in approximately 25% of the population [10–13,42]. The present study shows that the addictive drug nicotine produces a dynamic increase in cross correlations over time. Cross correlations did not increase significantly (using 5-ms binning) until well after the nicotine infusion, at which time the firing rate and burst activity had already peaked and reached a plateau. An increase in coincident spiking between neurons due to

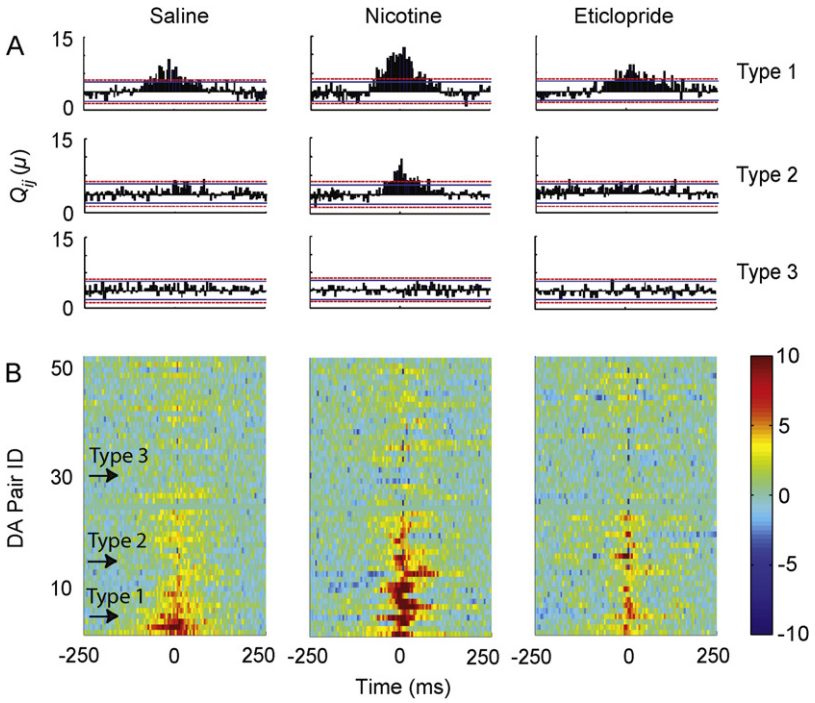

Fig. 4. Representative cross-covariance between different types of DA neuron pairs after saline (left), nicotine (middle), and eticlopride (right) administration. Cross correlograms were calculated for saline using 10 min of recording coming 5 min after saline infusion, for nicotine using 45 min of recording coming 15 min after nicotine infusion, and for eticlopride using 10 min of recording coming 5 min after eticlopride infusion. (A) Type 1 DA neurons displayed synchronizations at baseline (saline) and after nicotine. Type 2 DA neurons were only correlated after nicotine. Type 3 DA neurons showed no significant peak in either condition. The dotted red line indicates the 99.95% confidence interval that assumes independent neuron firing. If the cross-covariance, $Q_{ij}(\mu)$ rose above the confidence interval, the hypothesis of independent firing was rejected. (B) The pseudo-color plots show the $Q_{ij}(\mu)$ during saline, nicotine, and eticlopride arranged in ascending order for Type 1 to Type 2 to Type 3 DA neuron pairs (n = 52). Arrows indicate the position of the representative DA neuron pairs shown in panel A. Bin size = 5 ms and only 3 continuous bins above the confidence limit were treated as a significant peak to avoid any influence of noise. The pseudo-color code (10 to −10) for $Q_{ij}(\mu)$ is given to the right of the DA neuron pairs identified as 1–52.

a non-specific increase in their discharge frequency cannot explain these results. It was found that eticlopride (a DA D2-type receptor antagonist) enhanced the firing rate and burst activity of DA neurons to a greater degree than nicotine, but produced no increase in cross correlations. These and other observations suggest that the nicotine-induced increase in firing rate and in correlated DA neuron firing arise from mechanisms that are not necessarily identical. That is, the firing rate can increase substantially without inducing synchrony.

We hypothesize that different time courses of activation and desensitization of nAChR subtypes on GABA inputs to DA neurons could contribute to the delayed effect of nicotine on correlated firing. High affinity β2-containing nAChRs (likely in combination with α4 and α6) [43] serve a critical role in the regulation of DA neuron firing activity [5,7,44]. In vitro studies indicate that low concentrations of nicotine rapidly activate high affinity β2-containing nAChRs, but this activation is followed within minutes by significant desensitization and alteration of GABA and DA neuron function [4,35,45–47]. However, the time course of nicotine's action in vivo is not entirely understood, with nicotinic receptors fluctuating between the activated state and the desensitized state over an unknown period before reaching a relative steady-state, which may contribute to the delay in DA neuron synchronization.

DA neurons are under strong GABAergic control [48]. Therefore, changes in correlated activity between DA neurons could arise from shared inhibitory synaptic input arising from an intrinsic or extrinsic VTA source. Three observations from the present study are consistent with this possibility. The broad peak shape centered near zero in the cross correlograms matched those described for neurons coupled to a single inhibitory source [12,34]. Second, the initial infusion of nicotine often produced a transient excitation of GABA firing activity, which was anti-correlated with the gradual rising phase seen in DA neurons. This period was often followed by a stable phase of moderate excitation for both GABA and DA neurons, during which correlated DA neuron firing increased. Third, a minority subset of DA neuron pairs demonstrated obvious periodicity in their cross correlograms (see supplemental Fig. S1), suggesting rhythmic on and off inhibition. Other explanations are possible and cannot yet be excluded, such as common afferents to the pairs of DA neurons.

The correlation frequency computed by analyzing the 45 min period 15–60 min after nicotine administration was very close to the correlation computed by analyzing the 10 min period 30–40 min after nicotine (see supplemental Fig. S1). It is worth noting that the correlations during the first 15–30 min after nicotine were not different from the saline control period. Although longer recording periods (45 min) should provide more reliable estimates of the synchronizations induced by nicotine than shorter periods (15 min), these results suggest that shorter correlation periods are usable assuming that the DA neuron firing rates are stable. Therefore, studies that require a higher temporal resolution should consider using a sliding time window in their analysis to identify the optimal cross-correlation period.

Another issue to consider is that the cross covariance between spike trains is dependent on the bin size used to compute the correlations. The 5-ms bin size that we employ requires that two cells approach simultaneous spike activity [12]. Increasing the bin size would yield a greater proportion of correlations over the longer period. It is possible that larger bin sizes will reveal different kinds of correlations that are induced by nicotine.

It is unlikely that the population of putative DA neurons used in this analysis were misidentified. No single electrophysiological or pharmacological property is sufficient for identification, but in

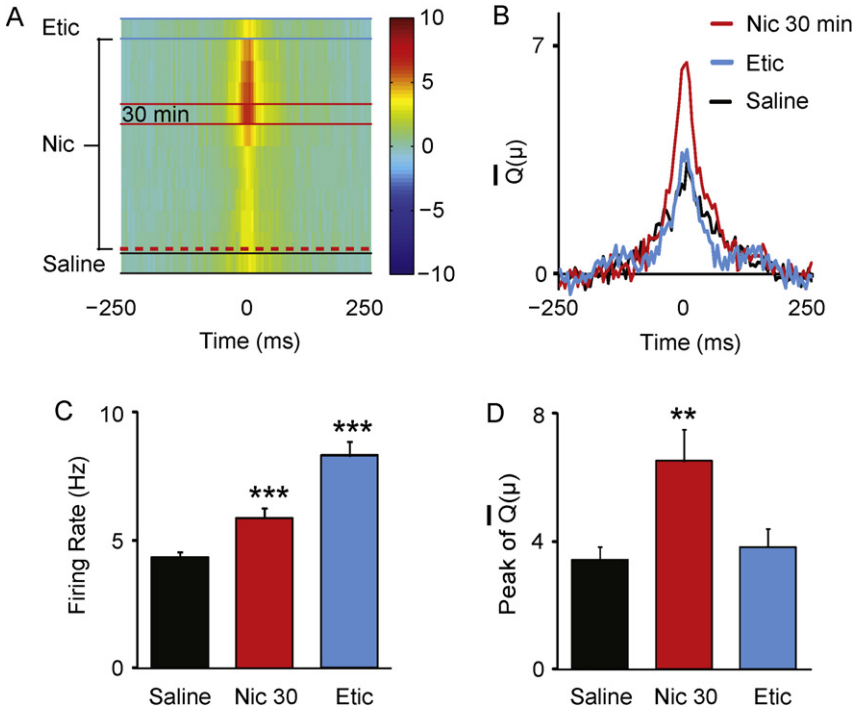

Fig. 5. Dynamic changes in cross correlations between DA neurons after nicotine administration. (A) The magnitude of the mean cross-covariance, $\bar{Q}(\mu)$ is denoted by the pseudo-color scheme (10 to −10) shown to the right. Each row denotes the mean cross covariance, $\bar{Q}(\mu)$ computed in a time window of 10 min along the length of in vivo recording (see Fig. 3). There are 12 $\bar{Q}(\mu)$ rows: 1 for saline (bottom row, between the black lines), 10 for nicotine beginning after nicotine administration indicated by the red dashed line, and 1 for eticlopride (top row, between the blue lines). The $\bar{Q}(\mu)$ rows are sorted in temporal order (during in vivo recording) from bottom to top. A $\bar{Q}(\mu)$ was not computed for the last 10-min window during the nicotine period. (B) Three $\bar{Q}(\mu)$ are shown during saline, nicotine (at the 30-min time window), and eticlopride for comparison. (C, D) Quantification of differences in firing rate and cross covariance within the 10-min window after saline infusion, 30 min after nicotine infusion, and after eticlopride infusion represented in panel A and B. Eticlopride enhanced the firing rate of DA neurons relative to saline, but it did not alter the strength of their correlations. $^{**}p < 0.01$ and $^{***}p < 0.001$ by paired t-test.

combination we isolated a subset of putative VTA DA neurons that clustered together across several dimensions and showed no consistent overlap with other non-DA VTA neurons. The putative DA neurons were distinguished from non-DA neurons by their D2-type pharmacological responses, their general waveforms, and the low variability in their firing rates, as indicated by the skew of the ISI distribution [20] (see Fig. 2B). This type of multi-dimensional within-group uniformity is not as likely to occur if the group constituted a mixed neuronal population.

These results are consistent with emerging views about the role of DA in reward based learning and memory processes [1,2,36]. An increase in correlated DA neuron firing across the VTA would amplify and synchronize the output of the DA signal at diverse target regions, such as the nucleus accumbens, prefrontal cortex, and hippocampus. Recent studies show that cues for conditioned (non-drug) rewards increase the synchronized spiking among DA neurons [10]. The DA signals to the hippocampus regulate perforant pathway long-term potentiation and conditioned behavior mediated by nicotine [18,49]. Correlations between neurons in the hippocampus and the prefrontal cortex occur during slow-wave sleep, a period essential for memory consolidation, and not during other sleep stages [50]. In addition, functional diversity between DA neurons in different subregions of the VTA continues to emerge [22,51–53]. Our results are consistent with recent studies showing that there are variations in the sensitivity of DA neurons to nicotine that vary with their location in the anterior and posterior VTA [9].

Taken together the present results provide significant evidence linking nicotine to functional connectivity among VTA DA neurons. An increase in DA output at mesostriatolimbic targets through a coordinated increase in DA neuron firing and burst activity would have an important impact on nicotine's reinforcing properties, including processes involved in learning and memory. Further studies of nicotine's effect on DA neuron firing patterns in the context of behavioral reinforcement would help to advance this prospect.

Acknowledgments

The authors are supported by grants from the National Institutes of Health, NIDA DA09411 and NINDS NS21229, and by the Cancer Prevention and Research Institute of Texas. The authors acknowledge the joint participation by Diana Helis Henry Medical Research Foundation through its direct engagement in the continuous active conduct of medical research in conjunction with Baylor College of Medicine and the Dopamine Signaling Dysfunction Precedes and Predicts Neuron Loss in an Animal Model of PD Project for the Parkinson's Program and the "Genomic, Neural, Preclinical Analysis for Smoking Cessation" Project for the Cancer Program.

Appendix A. Supplementary data

Supplementary data associated with this article can be found, in the online version, at doi:10.1016/j.bcp.2011.06.006.

References

[1] Berridge KC. The debate over dopamine's role in reward: the case for incentive salience. Psychopharmacology (Berl) 2007;191:391–431.
[2] Schultz W. Multiple dopamine functions at different time courses. Annu Rev Neurosci 2007;30:259–88.
[3] Grenhoff J, Aston-Jones G, Svensson TH. Nicotinic effects on the firing pattern of midbrain dopamine neurons. Acta Physiol Scand 1986;128:351–8.
[4] Pidoplichko VI, DeBiasi M, Williams JT, Dani JA. Nicotine activates and desensitizes midbrain dopamine neurons. Nature 1997;390:401–4.

[5] Schilstrom B, Rawal N, Mameli-Engvall M, Nomikos GG, Svensson TH. Dual effects of nicotine on dopamine neurons mediated by different nicotinic receptor subtypes. Int J Neuropsychopharmacol 2003;6:1–11.
[6] Zhang T, Zhang L, Liang Y, Siapas AG, Zhou FM, Dani JA. Dopamine signaling differences in the nucleus accumbens and dorsal striatum exploited by nicotine. J Neurosci 2009;29:4035–43.
[7] Mameli-Engvall M, Evrard A, Pons S, Maskos U, Svensson TH, Changeux JP, et al. Hierarchical control of dopamine neuron-firing patterns by nicotinic receptors. Neuron 2006;50:911–21.
[8] Dong Y, Zhang T, Li W, Doyon WM, Dani JA. Route of nicotine administration influences in vivo dopamine neuron activity: habituation, needle injection, and cannula infusion. J Mol Neurosci 2010;40:164–71.
[9] Zhao-Shea R, Liu L, Soll LG, Improgo MR, Meyers EE, McIntosh JM, et al. Nicotine-mediated activation of dopaminergic neurons in distinct regions of the ventral tegmental area. Neuropsychopharmacology 2011;36:1021–32.
[10] Joshua M, Adler A, Prut Y, Vaadia E, Wickens JR, Bergman H. Synchronization of midbrain dopaminergic neurons is enhanced by rewarding events. Neuron 2009;62:695–704.
[11] Wilson CJ, Young SJ, Groves PM. Statistical properties of neuronal spike trains in the substantia nigra: cell types and their interactions. Brain Res 1977;136:243–60.
[12] Hyland BI, Reynolds JN, Hay J, Perk CG, Miller R. Firing modes of midbrain dopamine cells in the freely moving rat. Neuroscience 2002;114:475–92.
[13] Morris G, Arkadir D, Nevet A, Vaadia E, Bergman H. Coincident but distinct messages of midbrain dopamine and striatal tonically active neurons. Neuron 2004;43:133–43.
[14] Van Bockstaele EJ, Pickel VM. GABA-containing neurons in the ventral tegmental area project to the nucleus accumbens in rat brain. Brain Res 1995;682:215–21.
[15] Steffensen SC, Svingos AL, Pickel VM, Henriksen SJ. Electrophysiological characterization of GABAergic neurons in the ventral tegmental area. J Neurosci 1998;18:8003–15.
[16] Carr DB, Sesack SR. GABA-containing neurons in the rat ventral tegmental area project to the prefrontal cortex. Synapse 2000;38:114–23.
[17] Omelchenko N, Sesack SR. Ultrastructural analysis of local collaterals of rat ventral tegmental area neurons: GABA phenotype and synapses onto dopamine and GABA cells. Synapse 2009;63:895–906.
[18] Tang J, Dani JA. Dopamine enables in vivo synaptic plasticity associated with the addictive drug nicotine. Neuron 2009;63:673–82.
[19] Clark D, Chiodo LA. Electrophysiological and pharmacological characterization of identified nigrostriatal and mesoaccumbens dopamine neurons in the rat. Synapse 1988;2:474–85.
[20] Margolis EB, Lock H, Hjelmstad GO, Fields HL. The ventral tegmental area revisited: is there an electrophysiological marker for dopaminergic neurons? J Physiol 2006;577:907–24.
[21] Margolis EB, Coker AR, Driscoll JR, Lemaitre AI, Fields HL. Reliability in the identification of midbrain dopamine neurons. PLoS One 2010;5:e15222.
[22] Lammel S, Hetzel A, Hackel O, Jones I, Liss B, Roeper J. Unique properties of mesoprefrontal neurons within a dual mesocorticolimbic dopamine system. Neuron 2008;57:760–73.
[23] Zhang TA, Placzek AN, Dani JA. In vitro identification and electrophysiological characterization of dopamine neurons in the ventral tegmental area. Neuropharmacology 2010;59:431–6.
[24] Grace AA, Bunney BS. The control of firing pattern in nigral dopamine neurons: burst firing. J Neurosci 1984;4:2877–90.
[25] Schwalger T, Fisch K, Benda J, Lindner B. How noisy adaptation of neurons shapes interspike interval histograms and correlations. PLoS Comput Biol 2010;6:e1001026.
[26] Perkel DH, Gerstein GL, Moore GP. Neuronal spike trains stochastic point processes. II. Simultaneous spike trains. Biophys J 1967;7:419–40.
[27] Brillinger D. Measuring the association of point processes: a case history. Am Math Mon 1976;83:16–22.
[28] Halliday D, Rosenberg J. Time and frequency domain analysis of spike train and time series data. In: Johansson UWH, editor. Modern Techniques in Neuroscience Research. Berlin: Springer-Verlag; 1999. p. 503–43.
[29] Siapas AG, Lubenov EV, Wilson MA. Prefrontal phase locking to hippocampal theta oscillations. Neuron 2005;46:141–51.
[30] Luo AH, Georges FE, Aston-Jones GS. Novel neurons in ventral tegmental area fire selectively during the active phase of the diurnal cycle. Eur J Neurosci 2008;27:408–22.
[31] Steffensen SC, Taylor SR, Horton ML, Barber EN, Lyle LT, Stobbs SH, et al. Cocaine disinhibits dopamine neurons in the ventral tegmental area via use-dependent blockade of GABA neuron voltage-sensitive sodium channels. Eur J Neurosci 2008;28:2028–40.
[32] Ikemoto S. Dopamine reward circuitry: two projection systems from the ventral midbrain to the nucleus accumbens-olfactory tubercle complex. Brain Res Rev 2007;56:27–78.
[33] Robinson S, Smith DM, Mizumori SJ, Palmiter RD. Firing properties of dopamine neurons in freely moving dopamine-deficient mice: effects of dopamine receptor activation and anesthesia. Proc Natl Acad Sci USA 2004;101:13329–34.
[34] Moore GP, Segundo JP, Perkel DH, Levitan H. Statistical signs of synaptic interaction in neurons. Biophys J 1970;10:876–900.
[35] Mansvelder HD, Keath JR, McGehee DS. Synaptic mechanisms underlie nicotine-induced excitability of brain reward areas. Neuron 2002;33:905–19.
[36] De Biasi M, Dani JA. Reward, addiction, withdrawal to nicotine. Annu Rev Neurosci 2011.
[37] Calabresi P, Lacey MG, North RA. Nicotinic excitation of rat ventral tegmental neurones in vitro studied by intracellular recording. Br J Pharmacol 1989;98:135–40.
[38] Picciotto MR, Zoli M, Rimondini R, Lena C, Marubio LM, Pich EM, et al. Acetylcholine receptors containing the beta2 subunit are involved in the reinforcing properties of nicotine. Nature 1998;391:173–7.
[39] Nashmi R, Xiao C, Deshpande P, McKinney S, Grady SR, Whiteaker P, et al. Chronic nicotine cell specifically upregulates functional alpha 4* nicotinic receptors: basis for both tolerance in midbrain and enhanced long-term potentiation in perforant path. J Neurosci 2007;27:8202–18.
[40] Exley R, Cragg SJ. Presynaptic nicotinic receptors: a dynamic and diverse cholinergic filter of striatal dopamine neurotransmission. Br J Pharmacol 2008;153(Suppl. 1):S283–97.
[41] Zhang L, Doyon WM, Clark JJ, Phillips PE, Dani JA. Controls of tonic and phasic dopamine transmission in the dorsal and ventral striatum. Mol Pharmacol 2009;76:396–404.
[42] Grace AA, Bunney BS. Intracellular and extracellular electrophysiology of nigral dopaminergic neurons—1. Identification and characterization. Neuroscience 1983;10:301–15.
[43] Exley R, Maubourguet N, David V, Eddine R, Evrard A, Pons S, et al. Distinct contributions of nicotinic acetylcholine receptor subunit {alpha}4 and subunit {alpha}6 to the reinforcing effects of nicotine. Proc Natl Acad Sci USA 2011;108:7577–82.
[44] Pidoplichko VI, Noguchi J, Areola OO, Liang Y, Peterson J, Zhang T, et al. Nicotinic cholinergic synaptic mechanisms in the ventral tegmental area contribute to nicotine addiction. Learn Mem 2004;11:60–9.
[45] Wooltorton JR, Pidoplichko VI, Broide RS, Dani JA. Differential desensitization and distribution of nicotinic acetylcholine receptor subtypes in midbrain dopamine areas. J Neurosci 2003;23:3176–85.
[46] Mansvelder HD, McGehee DS. Long-term potentiation of excitatory inputs to brain reward areas by nicotine. Neuron 2000;27:349–57.
[47] Mansvelder HD, McGehee DS. Cellular and synaptic mechanisms of nicotine addiction. J Neurobiol 2002;53:606–17.
[48] Grace AA, Floresco SB, Goto Y, Lodge DJ. Regulation of firing of dopaminergic neurons and control of goal-directed behaviors. Trends Neurosci 2007;30:220–7.
[49] Lisman JE, Grace AA. The hippocampal-VTA loop: controlling the entry of information into long-term memory. Neuron 2005;46:703–13.
[50] Wierzynski CM, Lubenov EV, Gu M, Siapas AG. State-dependent spike-timing relationships between hippocampal and prefrontal circuits during sleep. Neuron 2009;61:587–96.
[51] Chiodo LA, Bannon MJ, Grace AA, Roth RH, Bunney BS. Evidence for the absence of impulse-regulating somatodendritic and synthesis-modulating nerve terminal autoreceptors on subpopulations of mesocortical dopamine neurons. Neuroscience 1984;12:1–16.
[52] Hnasko TS, Chuhma N, Zhang H, Goh GY, Sulzer D, Palmiter RD, et al. Vesicular glutamate transport promotes dopamine storage and glutamate corelease in vivo. Neuron 2010;65:643–56.
[53] Stuber GD, Hnasko TS, Britt JP, Edwards RH, Bonci A. Dopaminergic terminals in the nucleus accumbens but not the dorsal striatum corelease glutamate. J Neurosci 2010;30:8229–33.
[54] Paxinos G, Watson C. The Rat Brain in Stereotaxic Coordinates. Burlington, MA: Academic Press; 2007.